J Neurophysiol 123: 1995–2009, 2020.
First published April 22, 2020; doi:10.1152/jn.00069.2020.

RESEARCH ARTICLE | *Sensory Processing*

Cortical processing of chemosensory and hedonic features of taste in active licking mice

Cecilia G. Bouaichi[1,2] and Roberto Vincis[1,2]
[1]*Department of Biological Science, Florida State University, Tallahassee, Florida; and* [2]*Program in Neuroscience, Florida State University, Tallahassee, Florida*

Submitted 18 February 2020; accepted in final form 15 April 2020

Bouaichi CG, Vincis R. Cortical processing of chemosensory and hedonic features of taste in active licking mice. *J Neurophysiol* 123: 1995–2009, 2020. First published April 22, 2020; doi:10.1152/jn.00069.2020.—In the last two decades, a considerable amount of work has been devoted to investigating the neural processing and dynamics of the primary taste cortex of rats. Surprisingly, much less information is available on cortical taste electrophysiology in awake mice, an animal model that is taking on a more prominent role in taste research. Here we present electrophysiological evidence demonstrating how the gustatory cortex (GC) encodes the basic taste qualities (sweet, salty, sour, and bitter) and water when stimuli are actively sampled through licking, the stereotyped behavior by which mice control the access of fluids in the mouth. Mice were trained to receive each stimulus on a fixed ratio schedule in which they had to lick a dry spout six times to receive a tastant on the seventh lick. Electrophysiological recordings confirmed that GC neurons encode both chemosensory and hedonic aspects of actively sampled tastants. In addition, our data revealed two other main findings: GC neurons rapidly encode information about taste qualities in as little as 120 ms, and nearly half of the recorded neurons exhibit spiking activity entrained to licking at rates up to 8 Hz. Overall, our results highlight how the GC of active licking mice rapidly encodes information about taste qualities as well as ongoing sampling behavior, expanding our knowledge on cortical taste processing.

NEW & NOTEWORTHY Relatively little information is available on the neural dynamics of taste processing in the mouse gustatory cortex (GC). In this study we investigate how the GC encodes chemosensory and palatability features of a wide panel of gustatory stimuli when actively sampled through licking. Our results show that GC neurons broadly encode basic taste qualities but also process taste hedonics and licking information in a temporally dynamic manner.

active licking; coding; extracellular recording; GC; gustation; taste

INTRODUCTION

The gustatory cortex (GC) is the primary cortical region responsible for processing taste information. Over the past decades, many studies have investigated the neural representation of gustatory stimuli in the GC of alert rats, an animal model that has been extensively used for the psychophysical examination of taste (Spector and Travers 2005). Electrophysiological analysis of spiking activity has revealed that the GC of rats encodes multiple facets of taste experience (Carleton et al. 2010; Maffei et al. 2012; Vincis and Fontanini 2016a), including the chemosensory (Katz et al. 2001; Stapleton et al. 2006) and hedonic (Grossman et al. 2008; Jezzini et al. 2013; Katz et al. 2001; Mukherjee et al. 2019) aspects of gustatory stimuli, as well as the expectation of taste (Saddoris et al. 2009; Samuelsen et al. 2012; Stapleton et al. 2006; Vincis and Fontanini 2016b).

Relatively less work has been done in mice, an animal model that offers easier access to genetic tools to manipulate and visualize neuronal activity. Although a considerable number of studies have investigated either spatial features of cortical taste-evoked activity in vivo (Chen et al. 2011; Fletcher et al. 2017; Lavi et al. 2018; Livneh et al. 2017) or taste behavior (Graham et al. 2014; Peng et al. 2015), limited information is available on cortical taste electrophysiology in awake mice. One recent study described how GC neurons encoded gustatory information when taste stimuli were injected into the mouths of alert mice via intraoral cannulas (IOCs) (Levitan et al. 2019). Although IOCs provide a reliable and rapid method to deliver taste solutions, they add a degree of passivity to taste delivery and could potentially alter the sequence of events associated with neural processing of gustatory information (Roussin et al. 2012). Passive stimulation (like IOCs for taste stimuli) could indeed bypass crucial components of active experiences such as motor rhythms inherent to active sensing (i.e., sniffing for olfaction, whisking for somatosensation) known to drive neural activity in sensory regions and to shape sensory processing and perception (Roussin et al. 2012; Schroeder et al. 2010; Shusterman et al. 2011; Wachowiak 2011). Liquid gustatory stimuli are sensed by rodents through licking, a stereotyped behavior by which fluids are actively introduced in the mouth (Graham et al. 2014; Travers et al. 1997). However, several key issues regarding cortical taste processing in active licking mice remain largely unaddressed.

The first question revolves around the temporal evolution of taste-evoked neural representations. Previous experiments using IOCs showed that taste processing within the GC is characterized by a dynamic and time-varying modulation of the firing activity extending up to multiple seconds after stimulus delivery (Levitan et al. 2019). However, in active licking mice and rats, smaller posttaste intervals (up to 0.5 s) were used to evaluate the processing of chemosensory coding (Stapleton et al. 2006; Vincis et al. 2019). As a result, it is not known if and how gustatory information of the four basic taste qualities

Correspondence: R. Vincis (e-mail: rvincis@fsu.edu).

evolves over a longer time interval after taste detection by active licking mice.

The second question pertains to the processing of hedonic value (i.e., whether a taste is palatable or unpalatable). Previous data have indicated that GC neurons not only encode the chemosensory identity of tastants but also code for palatability, a feature emerging 0.5 s after stimulus detection (Katz et al. 2001; Levitan et al. 2019; Mukherjee et al. 2019). While these studies used a passive form of tastant delivery via IOCs, it is still unknown whether GC neurons do in fact encode hedonic value of tastants and in what temporal window this is occurring when actively sampled via licking.

To address these questions, we designed and conducted experiments to determine the electrophysiological features of cortical processing of the four basic taste qualities (sweet, salty, bitter, and sour) and water associated with active sensing in mice across a long poststimulus temporal window. Spiking activity was recorded from single GC neurons in mice permitted to freely lick to receive tastants. To separate neural activity evoked by the gustatory stimuli from electrophysiological correlates of sensory and motor aspects of licking, we *1*) trained the mice to receive each taste on a fixed ratio schedule and *2*) did not start recording neural activity until the licking pattern evoked by each gustatory stimulus was similar across a 1.5-s temporal window. As a result, the neural response evoked by the tastants could be compared with the one elicited by licking the dry spout before taste delivery. This also served to make sure that neural activity evoked by the distinct tastants would not be impacted by differences in taste-evoked licking variables such as interlick interval and lick numbers.

Overall, our results are consistent with previous experiments involving IOCs in both mice and rats, indicating that GC neurons recorded from active licking mice encode both the chemosensory and hedonic aspects of gustatory stimuli in a broad and temporally rich fashion. Additionally, our data provide two additional insights into GC processing in mice. First, the activity of cortical neurons that encode taste information can be modulated by, and coherent with, licking. Second, the temporal dynamics of taste responses are fast; opposing reports using IOCs, identity of all taste qualities is coded within 320 ms, and palatability information arises within 1 s after taste delivery. In summary, our data obtained from mice actively sensing a broad panel of gustatory stimuli significantly expand our knowledge on cortical taste processing.

MATERIALS AND METHODS

Experimental Subjects

The experiments in this study were performed on four male and two female wild-type C57BL/6J adult mice (10–20 wk old). Mice were purchased from The Jackson Laboratory (Bar Harbor, ME); upon arrival, mice were housed on a 12:12-h light-dark cycle and had ad libitum access to food and water. Experiments and training were performed during the light portion of the cycle. Six days before training began, mice were water restricted and maintained at 85% of their presurgical weight. All experiments were reviewed and approved by the Florida State University Institutional Animal Care and Use Committee (IACUC) under protocol no. 1824.

Surgery and Tetrode Implantation

Before surgery, mice were anesthetized with a mixture of ketamine-dexmedetomidine (13.3 mg/mL, 0.16 mg/mL). The depth of anesthesia was monitored regularly via inspection of breathing rate and whisking and periodically estimating the tail reflex. Anesthesia was maintained with supplemental ketamine (30% of the induction dose) as needed throughout the surgery. A heating pad (World Precision Instruments) was used to maintain body temperature at 35°C. After the achievement of surgical level of anesthesia, the animal's head was shaved, cleaned and disinfected (with iodine solution and 70% alcohol), and fixed on a stereotaxic holder. A first craniotomy was drilled above the left GC on the mouse's skull (AP: 1.2 mm, ML: 3.5 mm relative to bregma) to implant a movable bundle of eight tetrodes and one single reference wire (Sandvik-Kanthal, PX000004) with a final impedance of 200–300 kΩ for tetrodes and 20–30 kΩ for the reference wire. A second hole was drilled on top of the visual cortex, where a ground wire (A-M Systems, catalog no. 781000) was lowered ~300 μm below the brain surface. During surgery, the tetrodes and reference wires were lowered 1.2 mm below the cortical surface; they were further lowered ~200 μm before the first day of recording and ~80 μm after each recording session. Before implantation, tetrode wires were coated with a lipophilic fluorescent dye (DiI; Sigma-Aldrich), allowing us to visualize the final location of the tetrodes at the end of each experiment. Tetrodes, ground wires, and a head screw (for the purpose of head restraint) were cemented to the skull with dental acrylic. Animals were allowed to recover for a week before the water restriction regimen began. For 3 consecutive postsurgery days, we administered a subcutaneous injection of carprofen (5 mg/kg) to reduce pain and inflammation.

Taste Delivery System and Licking Detection

The taste delivery system consisted of five separate taste lines (4 for tastants and 1 for water) that converged at the tip of the licking spout. The licking spout contained independent polyimide tubes (MicroLumen, ID = 0.0142), each one connected to one taste line. Gustatory stimuli [sucrose (200 mM), NaCl (50 mM), citric acid (10 mM), and quinine (0.5 mM); from Sigma-Aldrich; further dissolved in water to reach the final concentration and presented at room temperature] and water were delivered via gravity by computer-controlled (Bpod; Sanworks) 12-V solenoid valves (LHDA1231115H; Lee Company) calibrated to deliver a 3-μL droplet of fluid (in the context of our rig, the opening times of the solenoid valves to deliver 3 μL of fluid ranged between 15 and 24 ms). Each lick was detected when the tongue crossed an infrared light beam (940 nm) positioned just in front of the drinking spout (see Fig. 2*A*). The beam was generated by a fiber-coupled LED (M940F1; Thorlabs) and received by a photodiode (SM05PD1A; Thorlabs). Lick and taste delivery time stamps were recorded and synchronized with neural data acquisition (Plexon system; see below for more details) and with a MATLAB-based control system designed for animal behavior measurements (Bpod; Sanworks).

Behavioral Apparatus and Training

Two weeks after full recovery from the surgery (i.e., no sign of distress, proper grooming, proper eating and drinking, return to presurgical weight), mice were placed on a water restriction regimen (1.5 mL/day). One week after the start of water restriction, mice were progressively habituated to be head-restrained in the recording rig. The initial duration of head-restraint sessions was short (~5 min), and duration gradually increased over days. The restraint apparatus consisted of a metal stage with an elevated clamp for securing the head bolt. The body of the mouse was covered with a semicircular plastic shelter. The recording sessions took place within a Faraday cage (type II 36X36X40H CleanBench; TMC), to accommodate the requirement

of electrophysiological recording. Mice were trained with a fixed ratio schedule, in which they learned to lick the dry spout a specific number of times to trigger the delivery of the taste. During training the number of dry spout licks was gradually increased from FR2 (taste stimulus delivered at the 2nd lick) to FR7 (taste stimulus delivered at the 7th lick) before starting the neural recording. The availability of the spout was signaled to the animal by a brief (50 ms) auditory cue. A single trial consisted of the delivery of one of the five gustatory stimuli followed by a 3-μL water rinse 7 $\pm$ 1 s after taste delivery. After the delivery of the rinse, an intertrial interval (ITI) of 6.5 $\pm$ 1.5 s separated two consecutive trials. Each recording session consisted of at least of 15 trials per tastant. Water was presented both as a stimulus and as a rinse. We used water as a stimulus because water-specific responses have been reported in taste receptor cells (Zocchi et al. 2017) as well as neurons in brain stem taste-related areas (Nakamura and Norgren 1991; Nishijo and Norgren 1990; Rosen et al. 2010), in the gustatory thalamus (Verhagen et al. 2003), and in the GC (de Araujo et al. 2003; Gutierrez et al. 2010).

Electrophysiological Recordings

Voltage signals from the tetrodes were acquired, digitized, and band-pass filtered with the Plexon OmniPlex system (Plexon, Dallas, TX) (sampling rate: 40 kHz). Single units were off-line sorted with a combination of template algorithms, cluster-cutting techniques, and examinations of interspike interval plots using Offline Sorter (Plexon, Dallas, TX). Neural data were analyzed with custom-written scripts in MATLAB (MathWorks, Inc., Natick, MA). Peristimulus time histograms (PSTHs) were plotted around the time of taste delivery. A bin size of 200 ms was used unless otherwise specified. Tetrode wires were implanted above the GC (AP: 1.2 mm, ML: 3.5 mm, DV: ~1.1/1.2 mm). Before the first recording session, tetrode bundles were lowered ~350 μm; after each recording session, tetrodes were further lowered ~80 μm in order to sample new GC neuron ensembles. Across 25 sessions, a total of 283 neurons were isolated from six mice (the average yield was 47 neurons per mouse and 10.4 neurons per session). The average spontaneous firing rate was 5.4 $\pm$ 0.3 spikes/s, and the average firing rates evoked by each of the stimuli used were 8.3 $\pm$ 0.71 spikes/s for sucrose, 8.5 $\pm$ 0.73 spikes/s for NaCl, 8.0 $\pm$ 0.70 spikes/s for citric acid, 8.2 $\pm$ 0.72 spikes/s for quinine, and 8.7 $\pm$ 0.77 spikes/s for water.

Analysis of Neural Data

Taste responsiveness. General responsiveness to a taste solution or water (referred to as taste responsiveness) was evaluated by analysis of the firing rate. This analysis provided a quantification of each neuron's responsiveness to an aqueous solution in the mouth and was performed by grouping together taste stimuli and water trials. A neuron was deemed taste responsive if the evoked spiking activity (averaged over 1.5 s after stimulus delivery) significantly differed from the baseline activity (averaged over 0.5 s before stimulus delivery) by Wilcoxon rank sum test. Single units with a significant increase in firing rate following the stimulus were deemed excitatory, whereas units with a significant decrease in activity were deemed inhibitory responsive neurons. Response latency and duration (see Fig. 4) for taste-responsive neurons were assessed as follows. After stimulus delivery, a sliding window of 100 ms was moved in 20-ms increments until the spiking activity (measured as firing rate) was 2.58 standard deviations above or below the average prestimulus firing rate (averaged over 0.5 s before stimulus delivery). Response latency was determined by the trailing edge of the first significant bin. Response duration was determined by the leading edge of the last significant bin that was preceded exclusively by significant bins.

Taste selectivity. To understand if the spiking activity of GC neurons contained information of specific gustatory stimuli, we quantified their taste selectivity. Taste selectivity was assessed by evaluating differences in either the magnitude or time course of the taste-evoked firing rate across the five stimuli. We employed a two-way ANOVA (taste identity $\times$ time course) (Jezzini et al. 2013; Levitan et al. 2019; Liu and Fontanini 2015; Samuelsen et al. 2012), using 250-ms bins in the 0 to 1.5 s posttaste time interval. A neuron was deemed taste selective if the taste identity main effect or the interaction term (taste identity $\times$ time course) was significant at $P < 0.01$.

Sharpness index and entropy. To further investigate the response profile of GC neurons, we used sharpness index (SI) (Rainer et al. 1998; Yoshida and Katz 2011) and entropy (H) (Smith and Travers 1979), two standard methods used to evaluate selectivity in taste physiology. SI was computed on the mean firing rate during the 1.5-s-wide interval after taste delivery and was defined as

$$\mathrm{SI} = \frac{n - \left(\sum \frac{\mathrm{Fr}_i}{\mathrm{FR}_b} \right)}{n - 1}$$

where Fr_i is the mean firing rate for each taste (i = 1–5), FR_b is the maximum firing rate among gustatory stimuli, and n is the total number of stimuli (n = 5). A SI of 1 indicated that a neuron responded to one stimulus (narrow tuning), and the value 0 indicated equal responses across stimuli (broad tuning). Entropy metric H was computed as previously described by Smith and Travers (1979):

$$H = -K \sum_{i=1}^{n} P_i \log P_i$$

where K is a constant (1.43 for 5 taste stimuli) and P is the proportional response to each gustatory stimulus (i). For this analysis, taste responses were obtained by subtracting the mean taste-evoked firing rate (over 1.5 s after taste delivery) from the mean firing rate preceding taste (over 0.5 s before taste delivery). To control for inhibitory responses, the absolute value of taste response was included in the analysis. P_i is the proportional response to each tastant. Overall, a low H indicated a narrowly tuned taste-selective neuron, whereas a high H indicated a broadly tuned taste-selective neuron.

Classification taste identity—population decoding. To understand how well the GC encodes information regarding the identity of gustatory stimuli and how taste information is processed across time, we used a population decoding approach (Meyers 2013). To this end we first constructed a pseudopopulation of GC neurons using taste-selective neurons recorded across different sessions (n = 60). We then generated a firing-rate matrix (trials $\times$ time bin) where the spike time stamps of each neuron (1 s before and 1.5 s after taste) were realigned to taste delivery, binned into 120-ms time bins, and normalized to Z score. To assess the amount of taste-related information, we used a "max correlation coefficient" classifier. Spike activity data contained in our matrix were divided into 10 "splits": 9 (training sets) were used by the classifier algorithm to "learn" the relationship between the pattern of neural activity and the different tastants; 1 split (testing set) was used to make predictions about which taste was delivered given the pattern of spiking activity. This process was repeated 10 times (each time using different training and testing splits) to compute the decoding accuracy, defined as the fraction of trials in which the classifier made correct taste predictions.

Palatability-related spiking activity and time course. To evaluate whether GC activity encoded palatability-related information, we used the palatability index (PI) (Jezzini et al. 2013). It is important to note that in order to compute the PI, we *1*) exclusively considered GC neurons deemed taste selective by previous analysis (see *Taste selectivity*) and *2*) considered spiking activity evoked by sucrose, NaCl, citric acid, and quinine [we choose not to include water to better compare our results with previous reports using the same analysis to extract palatability-related activity (Jezzini et al. 2013; Liu and Fontanini 2015; Piette et al. 2012)]. To build the PI we considered the time course of the difference of the PSTHs (250-ms bin) in response

to tastants of similar (sucrose-NaCl and citric acid-quinine) versus opposite (sucrose-quinine, sucrose-citric acid, quinine-NaCl, citric acid-NaCl) palatability. To avoid potential confounds introduced by differences in baseline and evoked firing rates across our pools of taste-selective neurons, we first normalized the PSTHs with a receiver operating characteristic (ROC) procedure (Cohen et al. 2012). With this method, the taste-evoked (from time 0 to 1.5 s, with time 0 representing taste delivery) firing rate in each time bin was normalized to the baseline spiking activity (from time −0.5 to 0 s). The normalized firing rate resulted in numbers ranging between 0 and 1; values larger than 0.5 indicated that the firing rate in that bin is above baseline, whereas values below 0.5 indicated that the firing rate is below baseline. After normalizing the firing rate, we then computed the PI. We first computed the absolute value of the log-likelihood ratio of the normalized firing rate for taste responses with similar ($<|LR|>_{same}$) and opposite ($<|LR|>_{opposite}$) hedonic values:

$$\langle |LR| \rangle_{same} = 0.5 \times \left(\left| \ln \frac{sucrose}{NaCl} \right| + \left| \ln \frac{quinine}{citric\ acid} \right| \right)$$

$$\langle |LR| \rangle_{opposite} = 0.25 \times \left(\left| \ln \frac{sucrose}{quinine} \right| + \left| \ln \frac{sucrose}{citric\ acid} \right| + \left| \ln \frac{NaCl}{citric\ acid} \right| + \left| \ln \frac{NaCl}{quinine} \right| \right)$$

Then we defined the PI as $<|LR|>_{opposite} - <|LR|>_{same}$. Positive PI values (in red in Fig. 9) suggested that a neuron responded similarly to tastants with similar palatability and differently to stimuli with opposite hedonic values. Negative PI (in blue in Fig. 9) values indicated the alternative scenario in which a neuron responded differently to stimuli of the same palatability and similarly to taste with different hedonic values. A taste-selective GC neuron was deemed palatable related if its PI value after taste delivery *1*) was positive and *2*) exceeded the mean + 6 × standard deviation of the PI values in the baseline.

Licking phase coherence. The coherence (C) between licking and neural activity (spikes) was computed with the "coherencyc" function of the Chronux 2.12 software package (http://chronux.org/) (Mitra and Bokil 2008). Multitaper coherence was calculated *1*) using licking and neural activity between −1 and 1.5 s (with 0 s being taste delivery; 1-ms bin); *2*) using tapers 1–3, and *3*) for a frequency range of 5–8 Hz [frequency band observed in freely licking behavior (Spector et al. 1998)]. To compute the confidence interval of the coherence and the significant threshold (α at 0.01%) we used a jackknife method (Gutierrez et al. 2010; Jarvis and Mitra 2001); a GC neuron was deemed licking coherent if its lower confidence interval (99%) crossed the significance threshold. To investigate how spikes were distributed across the licking cycle we performed a procedure called "warping" (Shusterman et al. 2011), in which the duration of each licking cycle was normalized and the time of each spike was transformed into lick phase coordinates (from 0 to 2π; see Fig. 7). Sixteen consecutive licking cycles (6 before taste or water stimulus and 10 after stimulus) were used (see Fig. 7).

Histology

At the end of the experiment, mice were terminally anesthetized and perfused transcardially with 30 ml of PBS followed by 30 ml of 4% paraformaldehyde (PFA). The brains were extracted and postfixed with PFA for 24 h, after which coronal brain slices (100 μm thick) containing the GC were sectioned with a vibratome (VT1000 S; Leica). To visualize the tetrodes' tracks, brain slices were counterstained with Hoechst 33342 (1:5,000 dilution, H3570; ThermoFisher, Waltham, MA) by standard techniques and mounted on glass slides. GC sections were viewed and acquired on a confocal microscope (Eclipse Ti2; Nikon).

RESULTS

To investigate how cortical neurons encode taste information in freely licking mice, we recorded ensembles of single units via movable bundles of tetrodes implanted unilaterally in the GC (Fig. 1). One potential challenge of electrophysiological recordings during active sensing is that mice have intrinsic preferences for different tastants. These preferences could result in unique licking patterns for each stimulus, a potential confound for the interpretation of electrophysiological differences. To address this issue, we trained the mice to produce comparable numbers of licks to each stimulus. After habituation to head restraint, water-deprived mice were engaged in a FR7 task in which they had to lick 6 times to a dry spout to obtain a 3-μL drop of one of five gustatory stimuli (sucrose, 200 mM; NaCl, 50 mM; citric acid, 10 mM; quinine, 0.5 mM; water) (Fig. 2). Mice were trained until the licking pattern evoked by each of the individual gustatory stimuli was similar across a 1.5-s temporal epoch following taste delivery (Fig. 2*C*). Indeed, no statistical differences in the distribution of total lick number [Fig. 2*D*, *left*; 1-way ANOVA, $F(4) = 0.13$; $P = 0.97$] and interlick interval [Fig. 2*D*, *right*; 1-way ANOVA, $F(4) = 1.49$; $P = 0.21$] were observed across tastants. The similarity in taste-evoked licking ensured that differences in neural responses across gustatory stimuli within 1.5 s after taste delivery could not be attributed to sensorimotor sources.

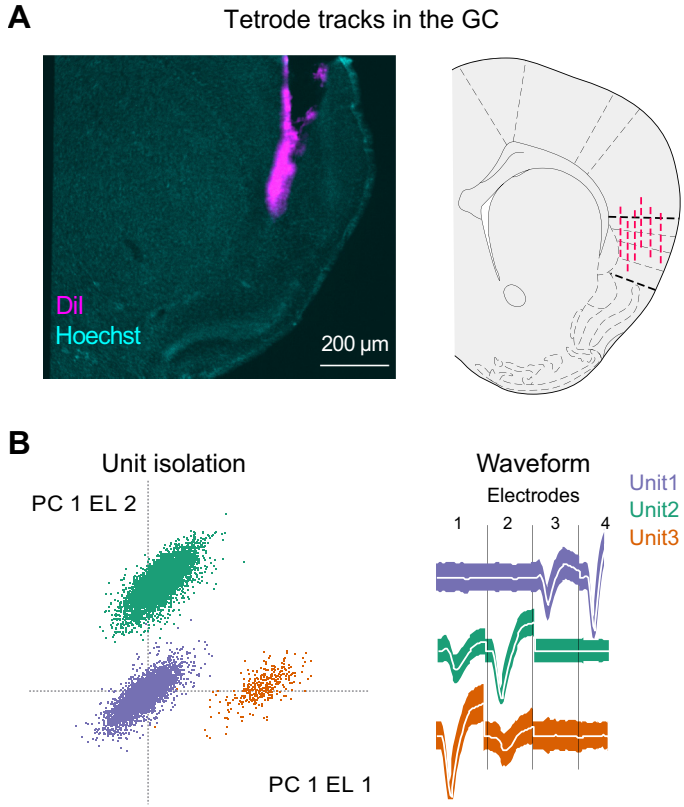

Fig. 1. Tetrode placement and single neuron recording. *A, left*: example of histological section showing the tetrode tracks (magenta) in the left gustatory cortex (GC). *Right*: schematic of the summary of the tetrode tracks from the 6 mice. *B, left*: representative single-unit recordings in the GC showing the principal component analysis of waveform shapes for spikes of 3 individual neurons. EL, electrode; PC, principal component. *Right*: average single-unit spike responses for the same 3 neurons, recorded from the 4 electrodes.

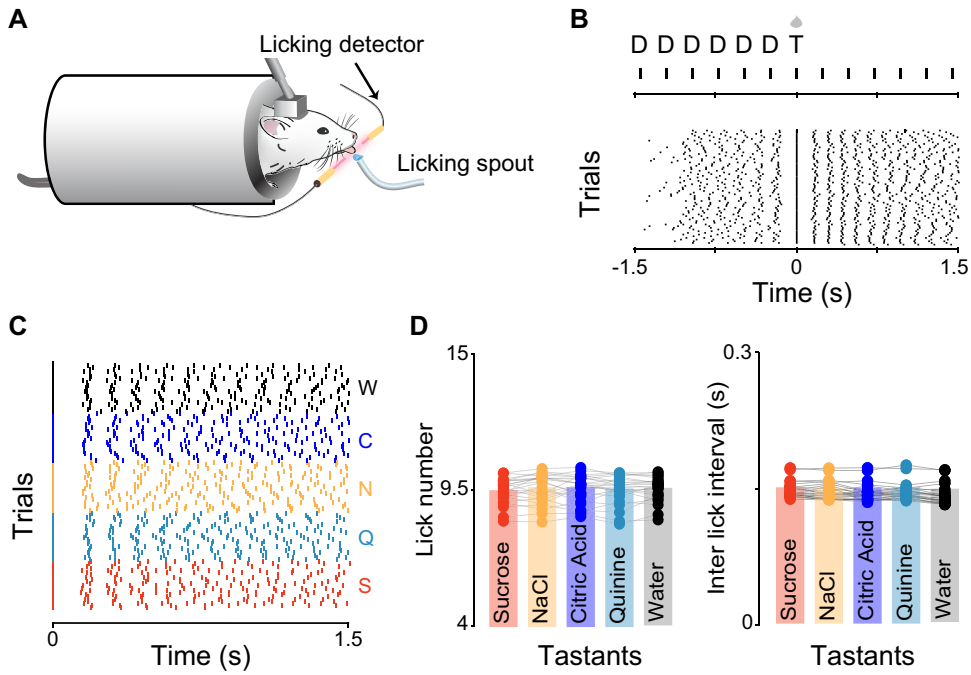

Fig. 2. Experimental design and taste-evoked licking pattern. *A*: sketch showing a head-restrained mouse licking a spout to obtain gustatory stimuli. *B*, *top*: diagram of the taste delivery paradigm. Gustatory stimuli (T) are delivered after 6 consecutive dry licks (D) to the spout. Each lick is symbolized by a vertical line. *Bottom:* raster plot of licking activity in 3-s time interval around taste delivery from 1 experimental session. Licking activity is realigned to stimulus delivery (*time 0* along the *x*-axis). *C*: raster plot of taste-evoked licking activity. Each line represents an individual lick; trials pertaining to different tastants are grouped together and color-coded, with sucrose (S) in red, quinine (Q) in cyan, NaCl (N) in yellow, citric acid (C) in blue, and water (W) in black. *D*, *left*: bar plots showing the number of licks evoked by each gustatory stimulus in a 1.5-s time interval after stimulus. *Right*: bar plots showing the interlick intervals (ILIs) for the licking pattern evoked by each tastant in a 1.5-s time interval after stimulus. Bars represent the mean, and each round point represents the individual lick number and ILI value extracted for the 25 experimental sessions analyzed.

Taste-Evoked Responses in Active Licking Mice

To begin evaluating the neural dynamics evoked by gustatory stimuli in active licking mice, we analyzed the spiking profile of single GC neurons. Figure 3 shows the raster plots and peristimulus time histograms (PSTHs) of three representative GC neurons. Visual inspection of the graphs indicates that each of these neurons is modulated by different gustatory stimuli in a temporally rich and dynamic manner.

As a first step, we wanted to understand how many GC neurons were modulated by the presence of a solution in the mouth. To this end, we compared the firing rate during baseline (averaged between −0.5 and 0 s, with 0 s being taste delivery) to the spiking activity (averaged between 0 and 1.5 s) evoked by the four gustatory stimuli (sucrose, NaCl, citric acid, quinine) and water. Wilcoxon rank sum analysis revealed that a substantial number of the recorded GC neurons [67% (190/283)] responded to at least one of the four chemical stimuli or water and were classified as "taste-responsive" (Fig. 4*A*). All other neurons [33% (93/283)] were classified as "non-taste-responsive" (Fig. 4*A*). It is important to note that taste-responsive neurons include GC neurons responding specifically to stimulus identity (i.e., GC neurons that do not respond to all 5 stimuli) as well as single units displaying nonspecific responses common to all stimuli (see next paragraph for further analysis). We observed that 56% (108/190) of taste-responsive neurons displayed an excitatory response (taste-evoked firing rate > baseline firing rate), whereas 43% (82/190) displayed an inhibitory response (taste-evoked firing rate < baseline firing rate) (Fig. 4*A*). Figure 4*B* shows the population averages (population PSTHs) of the excitatory and inhibitory responses. Analysis of the distribution of the latency of the responses indicated that the majority of taste-responsive neurons showed a fast onset, with firing rate significantly changing from baseline within the first 300 ms after taste delivery (Fig. 4*C*; mean onset 0.26 ± 0.022 s). Analysis of the duration of the responses revealed that the distribution of significant firing rate modulation was heterogeneous over the entire 1.5-s posttaste time interval analyzed (mean duration 0.49 ± 0.032 s).

Interestingly, there were no differences detected regarding the onset and the duration of the responses for both excitatory and inhibitory stimulus-evoked firing rates (onset and duration: Kolmogorov–Smirnov tests, $P = 0.8$ and $P = 0.9$, respectively).

Taste Selectivity and Chemosensory Tuning of GC Neurons

To further understand how the GC discriminates gustatory information concerning the different taste qualities, we moved beyond the taste responsiveness analysis. In fact, a taste-responsive neuron (see definition above) could be modulated similarly by all stimuli, including water (see Fig. 6*C*, *center*), reflecting general somatosensory (i.e., the delivery of liquid in the mouth) or cognitive (expectation of a taste based on the FR7 protocol) elements rather than chemosensory-specific activity. We addressed this issue using the following analysis. For each taste-responsive neuron, we compared the spiking activity evoked by the five different gustatory stimuli. Briefly, poststimulus (0–1.5 s) firing rate was divided into six 250-ms bins, and a two-way ANOVA was used with "taste stimuli" and "time" as variables (Jezzini et al. 2013; Levitan et al. 2019). Taste-responsive neurons that had significantly different responses to the five tastants in either the main effect "taste stimuli" or the "taste stimuli" × "time" interaction were defined as taste-selective. This method revealed that 31% (60/190) of taste-responsive neurons selectively encoded gustatory information, whereas the remaining (69%) likely encoded somatosensory or cognitive features.

Next, we evaluated the tuning profile of the taste-selective neurons. We aimed to understand if the taste-selective GC neurons recorded in active licking mice preferentially responded to only one single taste stimulus (i.e., narrow tuning) or if they were capable of encoding information pertaining to multiple tastes (i.e., broad tuning). Our analysis revealed that

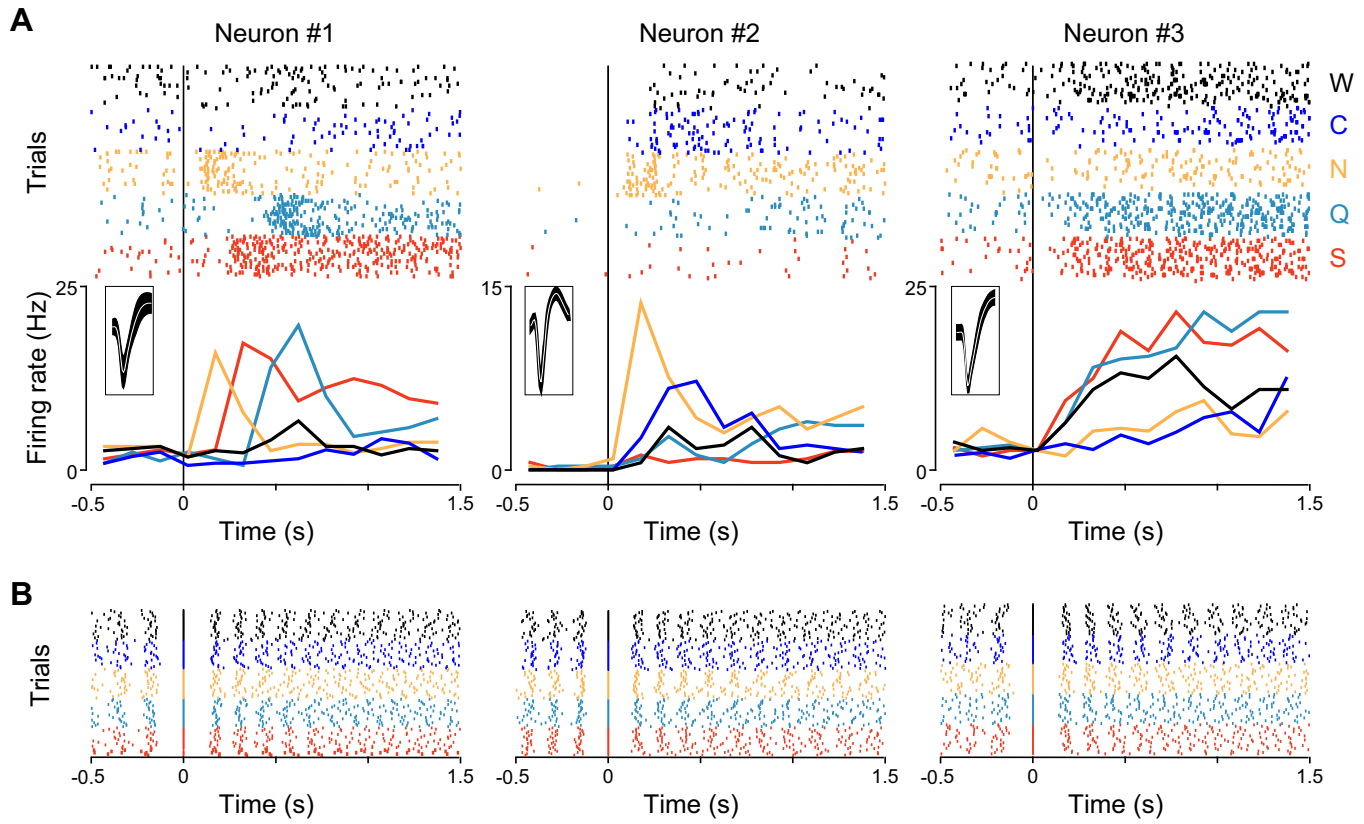

Fig. 3. Taste responses in active licking mice. *A*: raster plots and peristimulus time histograms (PSTHs) of 3 representative gustatory cortex neurons showing broadly tuned responses to the 5 stimuli. Vertical lines at *time 0* represent taste delivery. Trials pertaining to different tastants are grouped together (in the raster plots) and color-coded (both in the raster plots and PSTHs), with sucrose (S) in red, quinine (Q) in cyan, NaCl (N) in yellow, citric acid (C) in blue, and water (W) in black. *Insets*: average action potential waveforms for each of the 3 neurons. *B*: raster plots of taste-evoked licking activity from the experimental sessions where the neurons shown in *A* were recorded. Each line represents an individual lick; similar to *A*, trials pertaining to different tastants are grouped together and color-coded with, sucrose (S), quinine (Q), NaCl (N), citric acid (C), and water (W) in red, cyan, yellow, blue, and black, respectively.

21% of GC taste-selective neurons responded to one taste, 20% to two tastes, 23% to three and four tastes, and 11% to all stimuli (Fig. 4*E*, *left*). In addition, we observed that taste-selective neurons were not preferentially tuned to encode information pertaining to individual taste quality, but rather they broadly responded to gustatory stimuli independent of their chemical identity (Fig. 4*E*, *right*). To further investigate differences in the tuning profiles of GC neurons, we performed two additional analyses: we computed the response entropy (*H*) and the response sharpness index (SI) for each taste-selective neuron, two standard techniques used to evaluate the breadth of tuning of single neurons (Smith and Travers 1979; Wilson and Lemon 2013; Yoshida and Katz 2011). Figure 5*A* shows the distribution of *H* values of the taste-selective neurons. Low *H* values are evidence of narrowly tuned neurons (i.e., GC neurons that encode 1 taste stimulus; see *neuron 1* in Fig. 5*B*), whereas high *H* values indicate broadly tuned neurons (i.e., GC neurons that encode multiple taste stimuli; see *neuron 2* in Fig. 5*B* and the 3 neurons in Fig. 3). The distribution of *H* values strongly implies that the majority of taste-selective neurons are broadly tuned, suggesting that the bulk of taste-selective neurons in GC encode information of more than one taste. Similar results were obtained analyzing the response SI (Yoshida and Katz 2011). A SI of 1 describes a neuron responding to only one taste, and a SI of 0 describes a neuron responsive to all five gustatory stimuli. The results of this analysis further confirmed that GC neurons are broadly tuned, with an average SI of 0.34 ± 0.02 (data not shown).

Altogether our analyses revealed that 30% of GC neurons in active licking mice were capable of selectively encoding taste identity information. In addition, we showed that the majority of these neurons displayed a broadly tuned profile, indicating that a single taste-selective neuron is likely to process information of different gustatory stimuli.

Licking-Coherent Neurons

Electrophysiological studies performed in rats have indicated that neurons in the GC can integrate somatosensory and motor activity linked to licking (Gutierrez et al. 2010; Stapleton et al. 2006). To determine how rhythmic licking impacted neural activity in the mouse GC, we quantified the number of neurons that exhibited neural activity coherent with licking. In our analysis, coherence (C) revealed how well the spiking activity of one neuron was correlated with rhythmic licking in the 5–8 Hz frequency domain (see MATERIALS AND METHODS for further details). This analysis revealed that a substantial amount of GC neurons (137/283, 48.4% referred to hereafter as licking-coherent; Fig. 6*A*) exhibited spiking activity time-locked and correlated to subsequent licks in both frequency and phase. We examined whether the licking-coherent neurons were exclusively modulated by lick-related activity or if they also encoded taste-related chemosensory information. Addi-

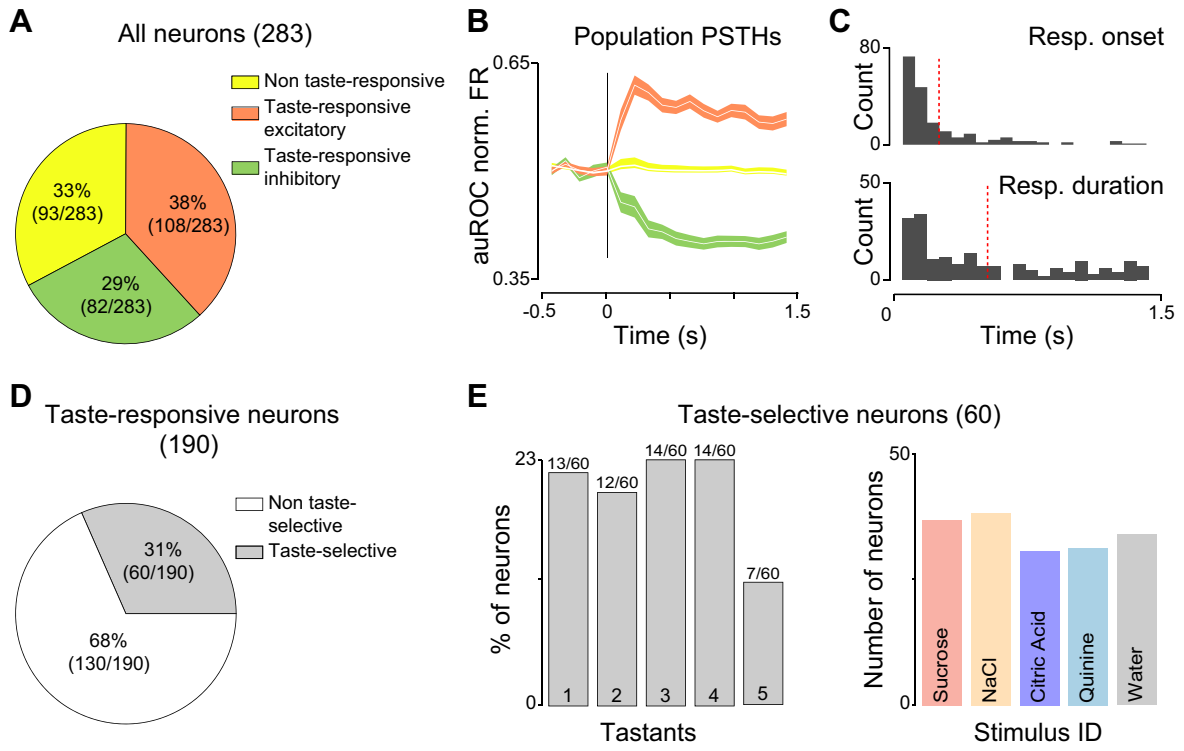

Fig. 4. Quantification of taste responses in the mouse gustatory cortex. *A*: pie chart displaying the proportion and distribution of neurons showing either an excitatory or inhibitory response to taste stimuli. *B*: population peristimulus time histograms (PSTHs) of excitatory (orange), inhibitory (green), and nonresponsive (yellow) neurons expressed as normalized firing rate (norm. FR). Shaded areas represent SE. auROC, area under the receiver operating characteristic curve. *C*: distribution of taste-evoked response onset (*top*) and response duration (*bottom*). Vertical red dotted lines represent mean values. *D:* pie chart showing the proportion of taste-responsive neurons that respond selectively to 1 or more tastant. Taste selectivity was assessed with 2-way ANOVA comparing responses to the different gustatory stimuli as a function of time. *E*: fraction of taste-selective neurons encoding 1, 2, 3, 4, or 5 gustatory stimuli (*left*) and number of taste-selective neurons responding to the 4 different taste qualities and water (*right*).

tional analyses on the firing rate modulation before and after taste delivery revealed three types of licking-coherent neurons (Fig. 6*B*). Forty-seven of 137 (34.3%) total licking-coherent neurons (Fig. 6*C*, *left*; licking-coherent only) displayed a rhythmic and lick-sensitive spiking activity with no differences in the firing rates evoked by licks preceding and following taste delivery and across tastants. These neurons likely exclusively encode somatosensory and/or motor aspects of licking and do

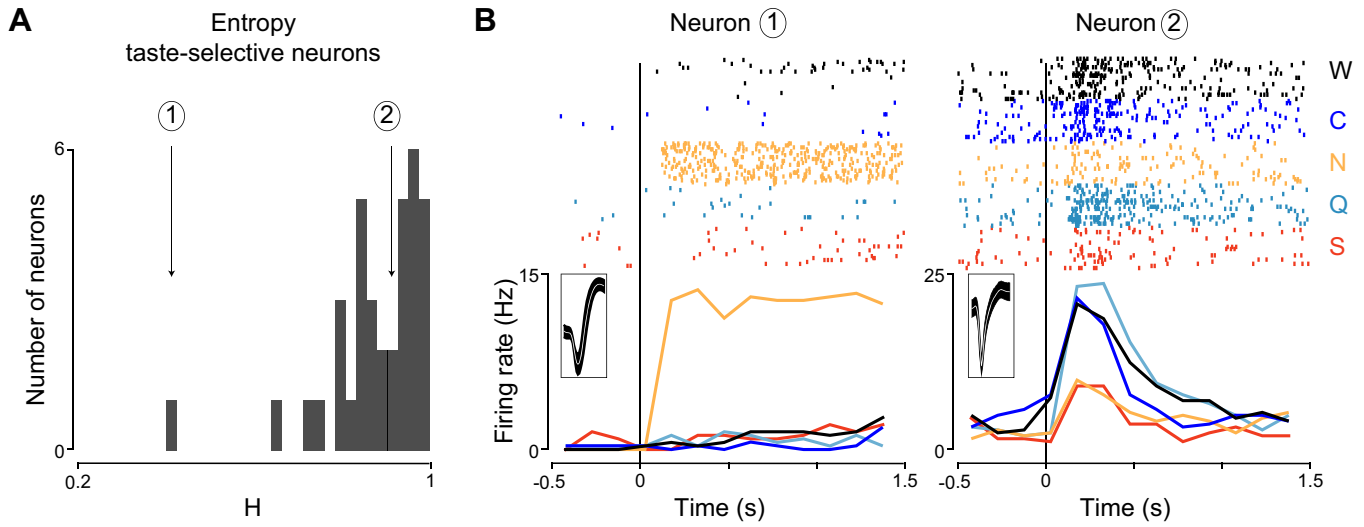

Fig. 5. Tuning of taste-selective neurons in the gustatory cortex (GC) of active licking mice. *A*: distribution of the breadth of tuning (expressed as entropy, *H*) of the taste-selective neurons. Low *H* values indicate narrowly responsive neurons, whereas high *H* values imply that the same neuron is modulated by multiple tastants. The distribution of *H* values is skewed to the right (toward high *H* values), indicating that the majority of taste-specific GC neurons are broadly tuned. Black arrows indicate the *H* values of the 2 representative neurons shown in *B*. *B*: raster plots and peristimulus time histograms (PSTHs) of 1 narrowly tuned (*neuron 1*) and 1 broadly tuned (*neuron 2*) GC neuron. Vertical lines at *time 0* represent taste delivery. Trials pertaining to different tastants are grouped together (in the raster plots) and color-coded (both in the raster plots and PSTHs), with sucrose (S), quinine (Q), NaCl (N), citric acid (C), and water (W) in red, cyan, yellow, blue, and black, respectively. *Insets*: average spike waveforms for *neurons 1* and *2*.

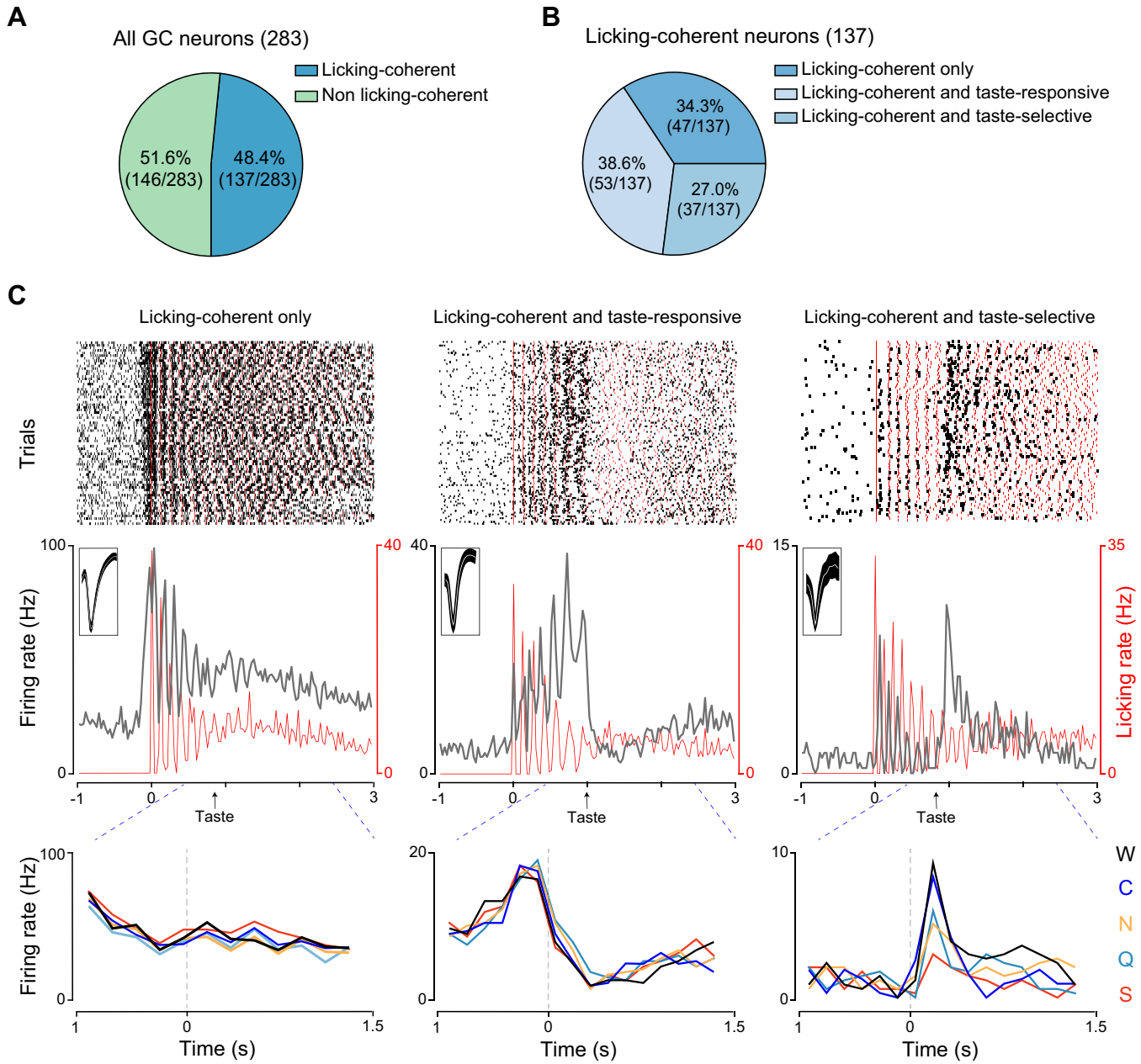

Fig. 6. Licking activity in the mouse gustatory cortex (GC). *A*: pie chart showing the proportion and distribution of GC neurons displaying licking-coherent activity. Note that neurons were defined as licking-coherent if they showed significant coherence between licking and neural activity in a temporal window spanning −1 and 1.5 s (with taste delivery at 0 s). *B*: pie chart displaying the proportion of licking-coherent neurons that were also defined as taste-responsive and taste-selective. *C*: raster plots and peristimulus time histograms (PSTHs) of 3 representative licking-coherent GC neurons: a "licking-coherent only" neuron (*left*), a "licking-coherent and taste-responsive" neuron (*center*), and a "licking-coherent and taste-specific" neuron (*right*). In the raster plots (*top*), each black line represents a spike and each red line represents a lick; note that in this case trials are not grouped based on the tastants, and neural and licking activities are realigned to the first dry lick. *Middle*: PSTHs represent the average firing (black line) and licking (red line) activity reported in the raster plot, binned in 50-ms time bins. Neural and licking activities are realigned to the first dry lick (*time 0* along the *x*-axis). The black arrow in the *x*-axis gives an estimate of when the taste stimulus was delivered. *Insets*: average spike waveforms. *Bottom*: PSTHs display the firing rate of the same 3 neurons. However, spiking activity is realigned to taste delivery (*time 0* and gray dashed line in the *x*-axis), color-coded based on the identity of the gustatory stimulus [sucrose (S) in red, quinine (Q) in cyan, NaCl (N) in yellow, citric acid (C) in blue, and water (W) in black] and binned in 200-ms time bins.

not integrate the information regarding the tactile inputs from fluid delivery in the oral cavity or the chemosensory identity of tastants. Fifty-three of 137 (38.6%) licking-coherent neurons (Fig. 6*C*, *center*; licking-coherent and taste-responsive) displayed a clear change in spiking activity following taste delivery but no differences across tastants. These neurons likely encode both somatosensory-motor features of licking and the presence of a taste solution in the mouth independent of taste quality and identity. The remaining 27% (37/137; Fig. 6*C*, *right*; licking-coherent and taste-selective) of neurons not only displayed lick- and taste-sensitive activity but also selectively discriminated the chemosensory identity of the tastants, evidenced by the two-way ANOVA analysis on their taste-evoked firing rate. A test for equality of proportion revealed that the

fractions of licking-coherent GC neurons are similar across the three types [licking-coherent only: 34.3% (47/137), licking-coherent and taste-responsive: 38.6% (53/137), and licking-coherent and taste-selective: 27.0% (37/137); proportion test: $\chi^2_2 = 4.29$; $P = 0.11$]. We then investigated whether the spiking activity of licking-coherent neurons was heterogeneously distributed across the lick cycle. Briefly, we normalized the duration of each licking cycle and transposed spike timing into lick phase coordinates, a procedure called warping (Shusterman et al. 2011). Figure 7*A* shows the raster plot of a licking-coherent neuron where spikes are plotted in lick phase coordinates for 16 consecutive licks. Visual inspection of the raster plot and analysis of the distribution of the spike count (Fig. 7*B*, *bottom*) indicated that this neuron tended to fire in the second half of the licking cycle. Further analysis, including all licking-coherent neurons, indicated that the lick-phase distribution of spikes was not heterogeneously distributed across the lick cycle (Rayleigh phase criterion for all licking-coherent neurons, $P < 0.001$). Interestingly, the distribution of spikes into lick phase coordinates for the three different groups of licking-coherent neurons (licking-coherent only, licking-coherent and taste-responsive, licking-coherent and taste-specific) shown in Fig. 6 (Fig. 7*C*) was not statistically different (circ_cmtest; licking-coherent only vs. licking-coherent and taste-responsive, $P = 0.12$; licking-coherent only vs. licking-coherent and taste-specific, $P = 0.56$; licking-coherent and taste-responsive vs. licking-coherent and taste-specific, $P = 0.85$).

Together, these results indicate that half of the neurons recorded in the GC of active licking mice are strongly correlated with licking activity, with neurons preferentially firing in between licks. Although the majority of these licking-coherent neurons are lick sensitive and encode somatosensory, yet chemosensory-independent, information of a fluid in the mouth, a substantial fraction was found to be taste selective. Indeed, analysis of the temporal dynamics of the taste-evoked firing rate in 1.5 s after taste delivery, revealed that 27% of licking coherent neurons also encode chemosensory information.

Population Decoding of Taste Information in Active Licking Mice

After characterizing the profile of the chemosensory and licking-related responses in single neurons, we focused our attention on the neural activity at population level. Although single-neuron activity can encode important features of sensory stimuli, information encoded in networks (population or ensemble) of neurons is used to inform behavioral choices. For

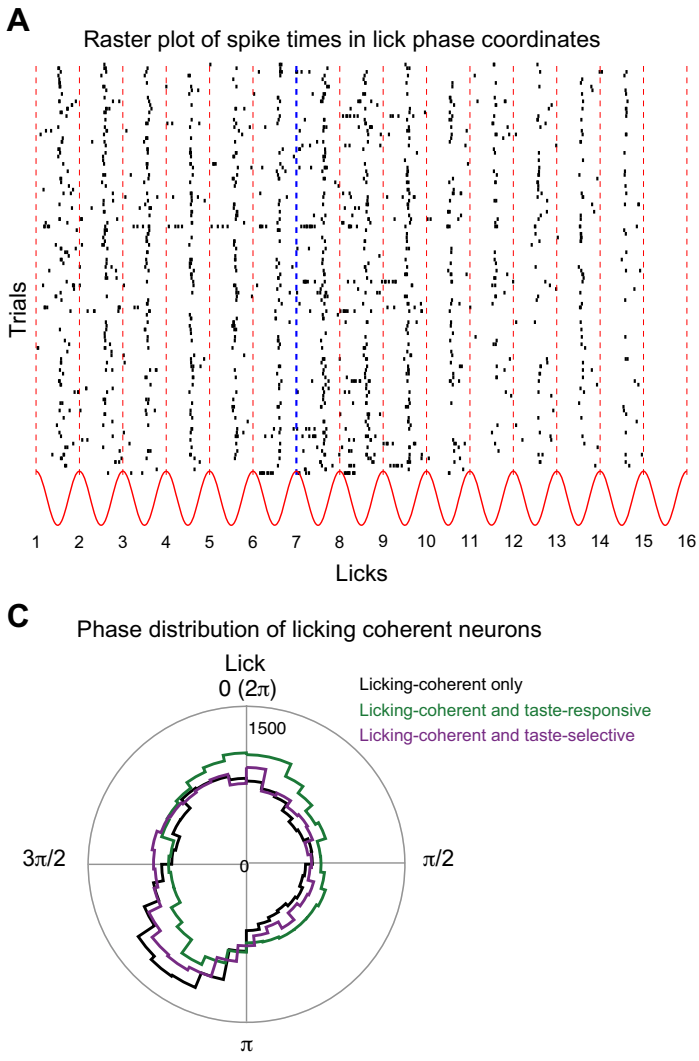

Fig. 7. Phase lick activity in the gustatory cortex. *A*: lick-warped raster plot of 1 representative licking-coherent neuron. Note that in this case trials are not grouped based on the tastes. *Lick 1* is the first lick to the dry spout, and *lick 7* is when 1 of the taste stimuli or water is delivered. Red and blue (7th lick that triggers taste delivery) dashed lines represent licks, and black ticks represent spikes. *B*, *top*: a sketch showing how phase lick coordinates were measured, where 0 and 2π signify consecutive licks and π indicates the time between licks. *Bottom*: distribution of spikes into lick phase coordinates for the representative neuron in *A*, showing that the majority of spikes occur between π and $3\pi/2$. *C*: distribution of spikes into lick phase coordinates for the 3 different groups of licking-coherent neurons shown in Fig. 6 (licking-coherent only in black, licking-coherent and taste-responsive in green, and licking-coherent and taste-selective in violet).

example, sudden changes in taste-evoked activity of GC neuron ensembles correlate with (Gutierrez et al. 2010; Stapleton et al. 2006), and are needed to drive (Mukherjee et al. 2019), behaviors (gapes in this case) aimed at expelling highly unpalatable tastants. Therefore, we used a population decoding analysis to quantify the gustatory information stored in the firing patterns of ensembles of GC neurons.

We computed the taste decoding performances in our taste-selective neurons (i.e., neurons whose firing rate selectively discriminated for the chemosensory identity of the tastants; $n = 60$; gold trace in Fig. 8*A*). The time course of the taste classification average across tastants is shown in Fig. 8*A*. Taste decoding showed an early onset (classification above chance from the first bin after taste delivery; Fig. 8*A*) and reached its peak ~500 ms after taste delivery (Fig. 8*A*). In addition, although the overall classification value started decreasing after 500 ms, decoding performances remained above chance until the end of the temporal window analyzed (Fig. 8*A*). As a control, the same analysis was performed with non-taste-selective neurons (neurons that responded to all gustatory stimuli similarly; see Fig. 6*C*, *center*, and Fig. 4*D*; $n = 130$; black trace in Fig. 8*A*). As expected, the taste classification accuracy never exceeded chance level (Fig. 8*A*). The time course of the classification analysis suggested that the spiking activity of GC neurons contained an optimal amount of information to discriminate the different gustatory stimuli in 500 ms (~4 licks) after taste delivery. However, it is well established that rodents are able to identify and discriminate specific taste qualities in a single lick (~120 ms) (Graham et al. 2014; Halpern and Tapper 1971; Stapleton et al. 2006, 2007). To evaluate taste decoding at a finer timescale, we constructed confusion matrices and characterized the classification performance for each taste in 120-ms time bins around taste delivery (Fig. 8*B*). As Fig. 8*A* shows, the average decoding performance in taste-selective neurons is well above chance (20%; black line in color bar in Fig. 8*B*; dark yellow color) during the first lick (between 0 and 120 ms). However, inspection of the confusion matrices in Fig. 8*B* revealed that in this early phase of taste processing not all taste stimuli are equally classified ($\chi^2_4 = 63.36$; $P < 0.001$). In this plot, the main diagonal highlights the fraction of trials in which the classifier correctly assigned the taste stimulus (predicted taste) to its real category (true taste). Comparison of the fraction of trials correctly classified for each individual tastant in the first 120 ms revealed that NaCl is the tastant best predicted by the decoding algorithm (Marascuilo's test, $P < 0.01$). As time progressed, all gustatory stimuli were similarly decoded with >40% accuracy (well above chance, which is 20%) within 320 ms ($\chi^2_4 = 8.68$; $P = 0.07$).

Altogether, these data indicate that ensembles of GC neurons recorded from active licking mice reliably encoded chemosensory information up to 2 s after taste delivery. In addition, taste coding showed an early onset, with the time course of the population decoding performance rising above chance within the first lick (~120 ms).

Processing of Palatability-Related Taste Information in Active Licking Mice

Studies in both anesthetized and alert rodents revealed that GC neurons also encode information about taste palatability when tastants are delivered intraorally (Accolla and Carleton 2008; Jezzini et al. 2013; Katz et al. 2001; Levitan et al. 2019; Sadacca et al. 2012).

However, it is still unknown whether GC neurons are capable of encoding hedonic information when gustatory stimuli are actively sensed through licking. Visual inspection of spiking activity in Fig. 9 indicates the presence of palatability-related neurons (see also *neuron 2* in Fig. 5), with both raster plots and PSTHs highlighting the similarity of the firing rate evoked by tastants belonging to the same hedonic category. To quantify the numbers of GC neurons encoding palatability-

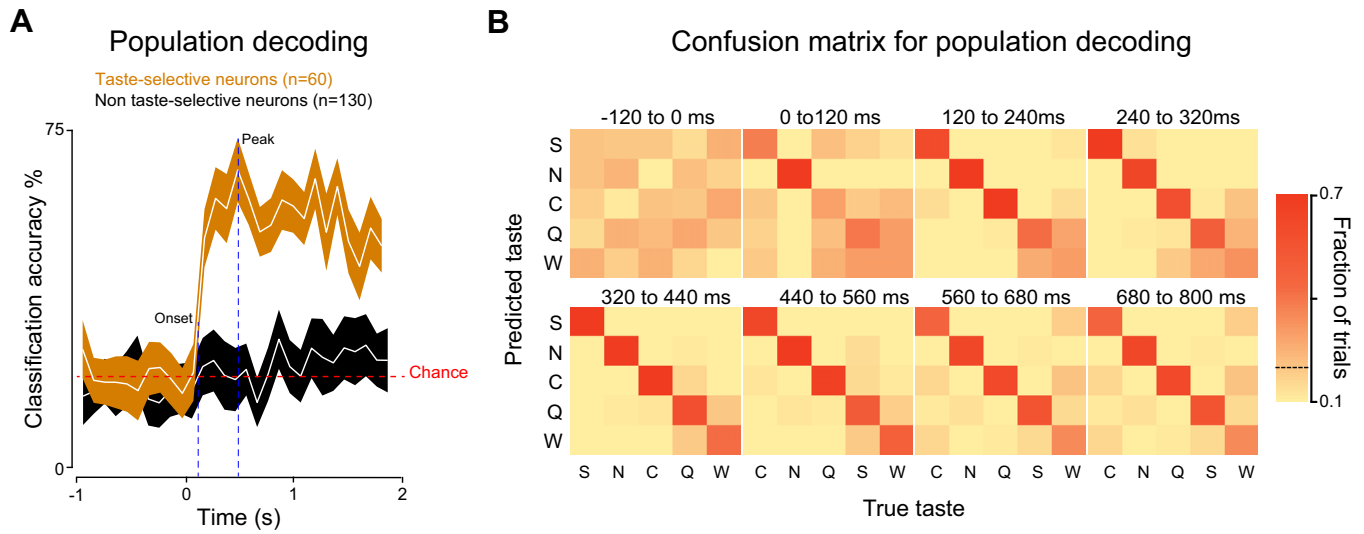

Fig. 8. Population decoding analysis and time course. *A*: time course of decoding performance considering the population of taste-selective (gold, $n = 60$) and nonselective (black, $n = 130$) neurons. Shading represents the bootstrapped confidence interval (CI), and red dashed line indicates chance-level performance (20%). *Time 0* indicates taste stimulus delivery. Blue vertical dashed lines indicate the onset and peak of decoding performance time course for the taste-selective neurons. Note that the temporal evolution of the spiking activity of the nonselective neurons (i.e., neurons that respond to all taste stimuli similarly; Fig. 6*C*, *center*, and Fig. 4*D*) does not convey information about taste. *B*: confusion matrix showing decoding performance for each gustatory stimulus in different 120-ms temporal windows around taste delivery (0 s). Color codes the classification accuracy, with darker hues indicating a higher fraction of correct trials. The main diagonal highlights the number of trials in which the classifier correctly assigned the taste stimulus (predicted taste) to its real category (true taste).

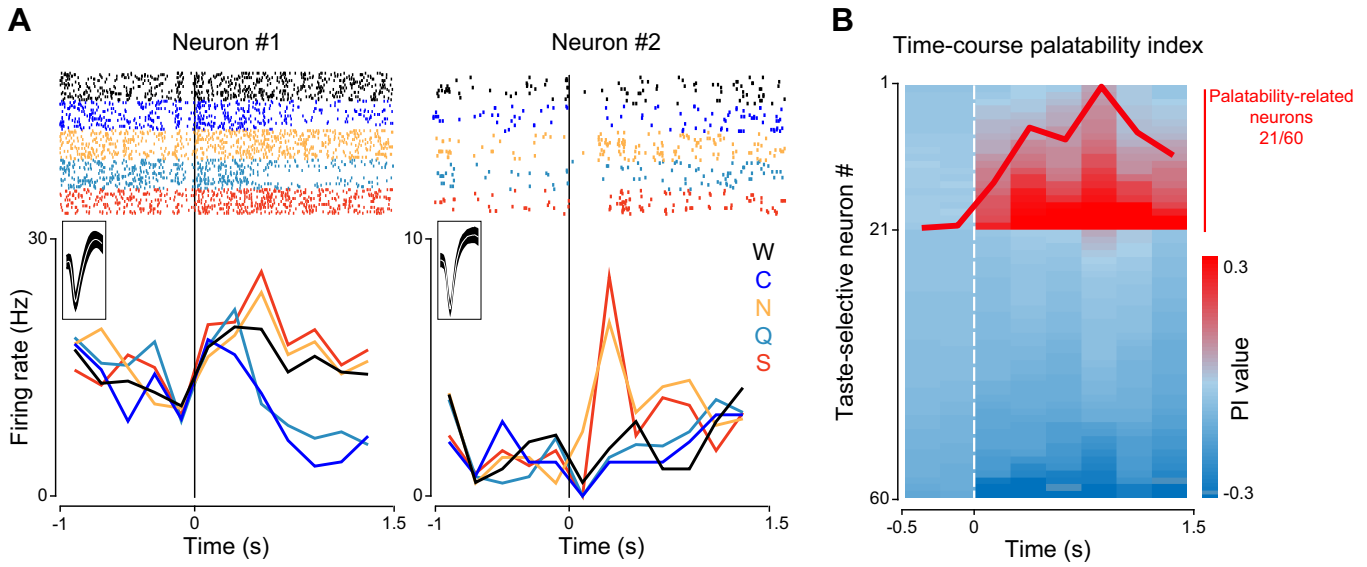

Fig. 9. Hedonic processing in the mouse gustatory cortex (GC). *A*: raster plots and peristimulus time histograms (PSTHs) of 2 neurons displaying palatability-related spiking activity. Vertical lines at *time 0* represent taste delivery. Trials pertaining to different tastants are grouped together (in the raster plots) and color-coded (in both the raster plots and PSTHs), with sucrose (S) in red, quinine (Q) in cyan, NaCl (N) in yellow, citric acid (C) in blue, and water (W) in black. *Insets*: average spike waveforms. *B*: color-coded plot showing the palatability index (PI) values across 2 s around taste delivery at 0 s for all 60 taste-selective neurons. Each row represents a single neuron; *time 0* and white vertical dashed lines highlight taste delivery. The thick red line superimposed on the color map represents the time course of the PI average value for the 21 taste-selective neurons that are deemed palatability related.

related features, we computed a palatability index (Jezzini et al. 2013; Liu and Fontanini 2015) (PI; see MATERIALS AND METHODS for further details). This analysis was based on extracting the taste response similarity for each taste-selective neuron (n = 60): positive PI values indicate palatability coding, and negative PI values imply inverse palatability coding (similar activity for tastants with opposite hedonic value and different activity for tastants with similar hedonic value). With this analysis, a neuron was deemed as encoding palatability if *1*) it had a positive PI value [it responded similarly to gustatory stimuli of similar hedonic value (sucrose-NaCl and citric acid-quinine) and differently to tastants with opposite palatability (sucrose-citric acid, sucrose-quinine, NaCl-quinine, and NaCl-citric acid)] and *2*) it had a PI significantly above baseline for at least 250 ms. This analysis revealed that 35% (21/60) of taste-selective neurons encoded hedonic value (Fig. 9*A*). To determine the temporal evolution of the neural processing of palatability, we analyzed the time course of the PI index (Fig. 9*B*). The thick red line overlying the heat map plot shows the PI averaged across palatability coding neurons. Palatability coding showed an early onset with two peaks (highest significant PI values): one before 500 ms and one before 1 s after taste delivery. As a control, the PI time course of taste-selective neurons not coding for hedonic values is also plotted and showed no modulation.

Overall, these results demonstrate that neurons in the mouse GC can encode taste palatability in addition to chemosensory identity. Interestingly, in active licking mice, GC hedonic coding emerges rapidly in the first second after taste delivery.

DISCUSSION

The results presented here provide evidence on how the gustatory cortex (GC) of mice encodes taste information when stimuli are sampled via active licking. Tetrode recordings revealed that GC neurons process information pertaining to the chemosensory identity of tastants in a temporally dynamic manner. Around 30% of the recorded neurons displayed taste-specific spiking activity, with the majority encoding for more than one taste. GC neurons also processed information of the hedonic value of tastants. Stimuli with similar palatability (i.e., sucrose and NaCl, citric acid and quinine) evoked similar firing activity in more than half of the taste-selective neurons. Analysis of the temporal sequence of both taste identity and hedonic value revealed that chemosensory information is encoded first, followed by palatability. Interestingly, coding of both features of gustatory stimuli occurred rapidly. Decoding population analysis revealed that taste identity started to be encoded during the first lick (within 120 ms after taste delivery) and palatability information arose and peaked within ~800 ms after taste delivery. Our data also revealed that the neural activity of nearly half of the GC neurons was coherent with licking, likely processing general tactile and motor activity. Notably, almost 30% of licking-coherent neurons were also taste specific, highlighting the capability of the GC to multiplex different features of taste experience.

Chemosensory and Palatability Neurons in the GC of Active Licking Mice

To date, only a handful of studies have investigated the electrophysiological profile and taste-evoked activity of the taste cortex in alert mice. Single-neuron spiking activity in response to gustatory stimuli has been examined in awake mice, either by using a limited set of tastants and focusing on a brief poststimulus interval (Kusumoto-Yoshida et al. 2015; Vincis et al. 2019) or by flushing taste stimuli directly in the oral cavity via surgically implanted intraoral cannulas (IOCs) (Levitan et al. 2019). This study represents the first electrophysiological investigation of the taste-evoked activity over a long poststimulus interval of GC neurons recorded from active licking mice.

Our experiments show that 66% of the recorded neurons were modulated by at least one taste, with a substantial fraction (31% of them; referred to as taste-selective neurons) capable of selectively encoding taste identity. Analysis of the breadth of tuning revealed that the majority of taste-selective neurons were broadly tuned, responding to more than one tastant. Most significantly, our results were in agreement with the conclusions reached in recent studies in which gustatory stimuli were delivered directly into the oral cavity. In fact, both in vivo calcium imaging (Fletcher et al. 2017; Livneh et al. 2017) and electrophysiological recordings from awake mice (Levitan et al. 2019) have indicated that a substantial fraction of GC neurons are modulated by gustatory stimuli and are likely to respond in a broadly tuned manner. It is also important to point out that our data on the breadth of tuning differ from two other studies in mice in which cortical taste responses were proposed to be narrowly tuned and confined within specific anatomical locations (Chen et al. 2011; Wang et al. 2018). On one hand, this discrepancy could largely arise from the differences in the neural activity readouts: calcium signals (used in Chen et al. 2011) represent only an indirect and partial measure of neural spiking (but see Fletcher et al. 2017; Livneh et al. 2017). On the other hand, these two studies investigated GC areas more rostral and/or caudal to the region we focused on. The possibility remains that more narrowly tuned neurons could be found at the anterior or posterior extremes of GC (but see Levitan et al. 2019).

Previous electrophysiological data have shown that GC neurons not only encode the physiochemical properties of tastants (i.e., their chemosensory identity) but also code for palatability (Katz et al. 2001; Levitan et al. 2019; Mukherjee et al. 2019). However, these studies used tastants delivered via IOCs. We evaluated whether GC neurons encode tastant hedonic value even when they are actively sampled via licking. It is important to note that as a consequence of our experimental design there are at least two caveats that can potentially mask palatability-related neural activity. First, compared with other studies (see Levitan et al. 2019), we used taste concentrations that were two times more diluted (at least for 3 of 4 tastants), thus reducing the range of palatability. Second, we recorded neural activity only from mice that displayed a taste-evoked licking microstructure (often used to behaviorally assess taste palatability) that was similar across stimuli after 7–10 days of training (see MATERIALS AND METHODS). Nevertheless, relying on a firing rate analysis method used extensively in the field (palatability index; Jezzini et al. 2013; Liu and Fontanini 2015; Piette et al. 2012), we determined that 35% of taste-selective neurons encode the hedonic value of the taste. Although our experiments were not directly designed to investigate variations in taste coding between rodent species (rats vs. mice) or taste delivery methods (IOCs vs. active licking), it is interesting to discuss similarities and potential differences. Our results suggest that the GC processes tastants similarly in both mice (this study) and rats, regardless of whether the tastants were actively sampled (this study) or delivered via IOCs (Jezzini et al. 2013; Katz et al. 2001; Levitan et al. 2019). Overall, GC neurons appear to use a common encoding strategy to process identity, including broadly tuned neurons, and palatability features of tastants regardless of rodent species and taste delivery methods (see *Temporal Processing of Taste Coding in Active Licking Mice* and *Lick-Related Neural Activity in the Mouse GC*, below).

Temporal Processing of Taste Coding in Active Licking Mice

Cortical taste processing is characterized by a dynamic and time-varying modulation of the firing activity of GC neurons (Katz et al. 2001). Various studies (in rats and mice) have extensively described and validated a model illustrating that taste responses evolve during multiple distinct temporal epochs in a 2-s time span following taste delivery (Grossman et al. 2008; Katz et al. 2001; Levitan et al. 2019). The first 200 ms were described as processing "general" tactile information of fluids contacting the oral cavity and were followed by two other temporal epochs in which chemosensory (200 ms to 1 s after stimulus delivery) and palatability (>1 s after stimulus delivery) features of taste were sequentially encoded. An outstanding question in the field is whether a similar temporal evolution of taste processing is observed during active sensing. Here we focused on the temporal dynamics of chemosensory coding. Population decoding revealed that GC neurons encode taste information in a single lick (Fig. 8). Our analysis indicated that the spiking activity of GC neurons contained sufficient information to discriminate among tastants in the first 120 ms after stimulus delivery.

Noteworthy to mention, although all tastants were classified with great accuracy (>50%) within the first 320 ms, the GC encoded NaCl with the shortest latency (~120 ms; Fig. 8*B*) and quinine with the longest latency (~320 ms; Fig. 8*B*), providing a compelling, additional argument that in the GC and in other subcortical taste regions taste-identity information of actively sampled stimuli can also be conveyed through temporal coding (Di Lorenzo et al. 2003; Di Lorenzo and Victor 2003; Rosen et al. 2011; Roussin et al. 2012; Stapleton et al. 2006, 2007). Interestingly, our decoding analysis data are also in agreement with a behavioral study that investigated the temporal features of taste quality perception in active licking mice (Graham et al. 2014). By performing a detailed analysis on the reaction times during a taste quality discrimination task, Graham et al. reported that certain taste qualities are perceived faster than others: NaCl was detected in a single lick, whereas quinine required multiple licking cycles. Therefore, thanks to the organization of the gustatory periphery (Breza et al. 2010; Roper 2013) and rhythmic licking behavior, it is tempting to speculate that the GC receives and integrates precise temporal sequences of spikes that could also provide taste-quality information leading to perception.

A careful evaluation of the decoding analysis presented in Fig. 8 indicates that taste-selective GC neurons are capable of discriminating water from the other four stimuli. Despite a long-standing debate over water as an independent taste modality, water-specific neural responses have been described in every region along the gustatory pathway (de Araujo et al. 2003; Nakamura and Norgren 1991; Nishijo and Norgren 1990; Rosen et al. 2010; Verhagen et al. 2003; Zocchi et al. 2017). Often these water responses are classified as somatosensory and discounted as not "taste mediated" (but see Rosen et al. 2010 and Zocchi et al. 2017), but our data argue against this view. Although some of the water responses can be accounted as purely somatosensory (see Fig. 6*C*, *center*), others cannot. The analyses presented in Fig. 8 suggest that the

spiking activity of taste-selective neurons contain sufficient "water-specific" information such that a pattern classifier can discriminate water from all the other taste stimuli (Fig. 8*B*). If all water responses were exclusively somatosensory (i.e., encoding common tactile inputs from all/some of the fluids delivered in the oral cavity), the decoding analysis would not be able to discriminate water from all the other tastes. Notably, water appeared to be the stimulus decoded with the longest latency, with the classification accuracy reaching values well above chance after 320 ms (Fig. 8*B*). Although understanding the exact cause of this latency will require more experiments, we can provide a parsimonious explanation. Considering that a certain amount of water is present in all taste stimuli (they are dissolved in water and used at low concentrations, see MATERIALS AND METHODS), a longer time might be needed by the GC to accumulate enough "water-specific" information so that the classifier can decode water against the other four stimuli.

Overall, our data indicate that GC neurons encode chemosensory information more rapidly when tastants are actively sampled through licking compared with when they are flushed passively into the mouth via IOCs (Katz et al. 2001). What could explain this difference? Tastants delivered via IOCs are often delivered to the mouth of the animal unexpectedly. In our experimental setting, the licking spout and the fixed-ratio paradigm could serve as anticipatory cues, allowing the animal to predict (i.e., expect) that a tastant would be delivered. Interestingly, a previous study has also shown that GC coding of gustatory stimuli can be expedited with anticipatory cues, priming the cortex for faster processing of chemosensory information (Samuelsen et al. 2012). This leads us to reason that actively sampled tastants are intrinsically expected, therefore prompting coding within the GC to occur faster than when tastants are unexpectedly delivered in the animal's mouth. Additionally, licking by itself could speed up GC taste processing (Graham et al. 2014). Our data indicate that almost half of GC neurons fire in synchrony and are phase locked with licking (Figs. 6 and 7). Thus, lick-induced rhythmic activity might facilitate GC taste processing with each lick cycle functioning as a "unit of gustatory processing" providing a fast, taste quality-dependent snapshot of the gustatory stimulus present in the mouth.

We then directed our attention to the time course of palatability coding. Further analysis of the temporal dynamics of taste-evoked firing rates reported overall rapid and persistent palatability processing. The time course of hedonic coding revealed two distinguishable palatability phases: a first "early" epoch that peaked at ~500 ms and a second "late" epoch peaking ~1 s after taste delivery. It is important to note that some of the GC neurons encoding palatability displayed both phases (like *neuron 2* in Fig. 9), suggesting that the GC produces two "waves" of hedonic information that can converge on the same neuron. Although the early phase of hedonic coding reported in our study precedes the appearance of palatability information obtained from neural recordings in the GC of rats (Jezzini et al. 2013; Katz et al. 2001), it does corroborate recent observations in the GC of mice receiving tastants passively from IOCs (Levitan et al. 2019). Overall, our experiments expand our knowledge on cortical taste processing, demonstrating that temporal multiplexing of chemosensory and hedonic gustatory information can be observed also in the context of mice sampling tastants via active licking.

One interesting point to discuss revolves around the behavioral relevance of the palatability-related activity. Many different studies have shown that basic licking and orofacial reactions—used as behavioral correlates of unconditioned taste hedonic value—are not altered after extended disruption of the GC (Hashimoto and Spector 2014; King et al. 2015), questioning the behavioral relevance of the GC palatability coding reported by many electrophysiological reports. Although the GC is likely not the only brain area involved in the generation of taste-driven hedonic reactions, it might play a temporally specific role in driving orofacial behavior. A recent report indicates that brief perturbation of GC around the time of the onset of the palatability-related activity significantly alters orofacial responses to quinine, suggesting that GC neurons might be instructive to produce normally timed orofacial responses (Mukherjee et al. 2019).

Lick-Related Neural Activity in the Mouse GC

Taste perception arises from the association between gustatory and oral-somatosensory information originating from receptors located in the oral cavity (Simon et al. 2006). The anatomical proximity and the neural connections between the gustatory and somatosensory cortices suggest that taste and oral somesthetic information could be intermingled in the cerebral cortex. Indeed, multiple studies in rats (Gutierrez et al. 2010; Katz et al. 2001; Stapleton et al. 2006) have shown that GC neurons displaying a characteristic firing rate in the 5–10 Hz frequency domain can process lick-related somatosensory activity. These results suggest that the majority of licking-coherent neurons fail to discriminate between the different tastes, suggesting that oral chemosensory and somatosensory information are processed by different groups of GC neurons. Our results expand upon this view. Almost half of the recorded neurons show firing patterns that are related to licking (licking-coherent neurons; Fig. 6). Analysis of the neural responses to licking activity and gustatory stimuli revealed that the majority of licking-coherent neurons (lick-coherent only, lick-coherent and taste-responsive; Fig. 6) failed to discriminate chemosensory information. As was already shown in subcortical taste-related brain areas (Roussin et al. 2012; Weiss et al. 2014), these neurons are likely conveying either rhythmic licking information or general intraoral tactile features and might collaborate with chemosensory neurons to identify and process taste information. However, our data indicate that not all of the GC licking-coherent neurons belong to the aforementioned category. Indeed, almost one-third of the neurons displaying spiking activity that correlated with licks also encoded taste information (lick-coherent and taste-selective; Fig. 6). Interestingly, all lick-related neurons showed the same preferred lick phase angle (Fig. 7). Analysis of the lick-phase distribution of spikes clearly indicates that the firing rate of the three different groups of licking-coherent neurons is preferentially locked to the same phase of the licking cycle (Fig. 7). Altogether, these observations argue against a clear demarcation between neurons that process chemosensory taste information and those integrating licking-related activity but rather support an alternative scenario. As already proposed by Denman et al. (2019) for the neurons in the nucleus of the solitary tract, the population of GC neurons showed a continuum with neurons that exclusively encode lick or taste activity at the extremes and

neurons capable of multiplexing different aspects of taste experience—integrating lick, tactile, and chemosensory information—in the middle. These observations strongly indicate licking as an integral part of the rodent taste experience and reaffirm the GC as one of the fundamental brain areas capable of integrating sensation and action pertaining to taste experience (Mukherjee et al. 2019; Vincis et al. 2019).

ACKNOWLEDGMENTS

The authors acknowledge Dr. Douglas Storace, Dr. Alfredo Fontanini, and the members of the Vincis laboratory for feedback and insightful comments.

GRANTS

This work has been supported by National Institute on Deafness and Other Communication Disorders Grant R21 DC-016714.

DISCLOSURES

No conflicts of interest, financial or otherwise, are declared by the authors.

AUTHOR CONTRIBUTIONS

R.V. conceived and designed research; C.G.B. and R.V. performed experiments; C.G.B. and R.V. analyzed data; R.V. interpreted results of experiments; R.V. prepared figures; C.G.B. and R.V. drafted manuscript; C.G.B. and R.V. edited and revised manuscript; C.G.B. and R.V. approved final version of manuscript.

REFERENCES

Accolla R, Carleton A. Internal body state influences topographical plasticity of sensory representations in the rat gustatory cortex. *Proc Natl Acad Sci USA* 105: 4010–4015, 2008. doi:10.1073/pnas.0708927105.

Breza JM, Nikonov AA, Contreras RJ. Response latency to lingual taste stimulation distinguishes neuron types within the geniculate ganglion. *J Neurophysiol* 103: 1771–1784, 2010. doi:10.1152/jn.00785.2009.

Carleton A, Accolla R, Simon SA. Coding in the mammalian gustatory system. *Trends Neurosci* 33: 326–334, 2010. doi:10.1016/j.tins.2010.04.002.

Chen X, Gabitto M, Peng Y, Ryba NJ, Zuker CS. A gustotopic map of taste qualities in the mammalian brain. *Science* 333: 1262–1266, 2011. doi:10.1126/science.1204076.

Cohen JY, Haesler S, Vong L, Lowell BB, Uchida N. Neuron-type-specific signals for reward and punishment in the ventral tegmental area. *Nature* 482: 85–88, 2012. doi:10.1038/nature10754.

de Araujo IE, Kringelbach ML, Rolls ET, McGlone F. Human cortical responses to water in the mouth, and the effects of thirst. *J Neurophysiol* 90: 1865–1876, 2003. doi:10.1152/jn.00297.2003.

Denman AJ, Sammons JD, Victor JD, Di Lorenzo PM. Heterogeneity of neuronal responses in the nucleus of the solitary tract suggests sensorimotor integration in the neural code for taste. *J Neurophysiol* 121: 634–645, 2019. doi:10.1152/jn.00578.2018.

Di Lorenzo PM, Hallock RM, Kennedy DP. Temporal coding of sensation: mimicking taste quality with electrical stimulation of the brain. *Behav Neurosci* 117: 1423–1433, 2003. doi:10.1037/0735-7044.117.6.1423.

Di Lorenzo PM, Victor JD. Taste response variability and temporal coding in the nucleus of the solitary tract of the rat. *J Neurophysiol* 90: 1418–1431, 2003. doi:10.1152/jn.00177.2003.

Fletcher ML, Ogg MC, Lu L, Ogg RJ, Boughter JD Jr. Overlapping representation of primary tastes in a defined region of the gustatory cortex. *J Neurosci* 37: 7595–7605, 2017. doi:10.1523/JNEUROSCI.0649-17.2017.

Graham DM, Sun C, Hill DL. Temporal signatures of taste quality driven by active sensing. *J Neurosci* 34: 7398–7411, 2014. doi:10.1523/JNEUROSCI.0213-14.2014.

Grossman SE, Fontanini A, Wieskopf JS, Katz DB. Learning-related plasticity of temporal coding in simultaneously recorded amygdala-cortical ensembles. *J Neurosci* 28: 2864–2873, 2008. doi:10.1523/JNEUROSCI.4063-07.2008.

Gutierrez R, Simon SA, Nicolelis MA. Licking-induced synchrony in the taste-reward circuit improves cue discrimination during learning. *J Neurosci* 30: 287–303, 2010. doi:10.1523/JNEUROSCI.0855-09.2010.

Halpern BP, Tapper DN. Taste stimuli: quality coding time. *Science* 171: 1256–1258, 1971. doi:10.1126/science.171.3977.1256.

Hashimoto K, Spector AC. Extensive lesions in the gustatory cortex in the rat do not disrupt the retention of a presurgically conditioned taste aversion and do not impair unconditioned concentration-dependent licking of sucrose and quinine. *Chem Senses* 39: 57–71, 2014. doi:10.1093/chemse/bjt054.

Jarvis MR, Mitra PP. Sampling properties of the spectrum and coherency of sequences of action potentials. *Neural Comput* 13: 717–749, 2001. doi:10.1162/089976601300014312.

Jezzini A, Mazzucato L, La Camera G, Fontanini A. Processing of hedonic and chemosensory features of taste in medial prefrontal and insular networks. *J Neurosci* 33: 18966–18978, 2013. doi:10.1523/JNEUROSCI.2974-13.2013.

Katz DB, Simon SA, Nicolelis MAL. Dynamic and multimodal responses of gustatory cortical neurons in awake rats. *J Neurosci* 21: 4478–4489, 2001. doi:10.1523/JNEUROSCI.21-12-04478.2001.

King CT, Hashimoto K, Blonde GD, Spector AC. Unconditioned oromotor taste reactivity elicited by sucrose and quinine is unaffected by extensive bilateral damage to the gustatory zone of the insular cortex in rats. *Brain Res* 1599: 9–19, 2015. doi:10.1016/j.brainres.2014.12.035.

Kusumoto-Yoshida I, Liu H, Chen BT, Fontanini A, Bonci A. Central role for the insular cortex in mediating conditioned responses to anticipatory cues. *Proc Natl Acad Sci USA* 112: 1190–1195, 2015. doi:10.1073/pnas.1416573112.

Lavi K, Jacobson GA, Rosenblum K, Lüthi A. Encoding of conditioned taste aversion in cortico-amygdala circuits. *Cell Reports* 24: 278–283, 2018. doi:10.1016/j.celrep.2018.06.053.

Levitan D, Lin JY, Wachutka J, Mukherjee N, Nelson SB, Katz DB. Single and population coding of taste in the gustatory cortex of awake mice. *J Neurophysiol* 122: 1342–1356, 2019. doi:10.1152/jn.00357.2019.

Liu H, Fontanini A. State dependency of chemosensory coding in the gustatory thalamus (VPMpc) of alert rats. *J Neurosci* 35: 15479–15491, 2015. doi:10.1523/JNEUROSCI.0839-15.2015.

Livneh Y, Ramesh RN, Burgess CR, Levandowski KM, Madara JC, Fenselau H, Goldey GJ, Diaz VE, Jikomes N, Resch JM, Lowell BB, Andermann ML. Homeostatic circuits selectively gate food cue responses in insular cortex. *Nature* 546: 611–616, 2017. doi:10.1038/nature22375.

Maffei A, Haley M, Fontanini A. Neural processing of gustatory information in insular circuits. *Curr Opin Neurobiol* 22: 709–716, 2012. doi:10.1016/j.conb.2012.04.001.

Meyers EM. The neural decoding toolbox. *Front Neuroinform* 7: 8, 2013. doi:10.3389/fninf.2013.00008.

Mitra P, Bokil H. *Observed Brain Dynamics*. Oxford, UK: Oxford Univ. Press, 2008.

Mukherjee N, Wachutka J, Katz DB. Impact of precisely-timed inhibition of gustatory cortex on taste behavior depends on single-trial ensemble dynamics. *eLife* 8: e45968, 2019. doi:10.7554/eLife.45968.

Nakamura K, Norgren R. Gustatory responses of neurons in the nucleus of the solitary tract of behaving rats. *J Neurophysiol* 66: 1232–1248, 1991. doi:10.1152/jn.1991.66.4.1232.

Nishijo H, Norgren R. Responses from parabrachial gustatory neurons in behaving rats. *J Neurophysiol* 63: 707–724, 1990. doi:10.1152/jn.1990.63.4.707.

Peng Y, Gillis-Smith S, Jin H, Tränkner D, Ryba NJ, Zuker CS. Sweet and bitter taste in the brain of awake behaving animals. *Nature* 527: 512–515, 2015. doi:10.1038/nature15763.

Piette CE, Baez-Santiago MA, Reid EE, Katz DB, Moran A. Inactivation of basolateral amygdala specifically eliminates palatability-related information in cortical sensory responses. *J Neurosci* 32: 9981–9991, 2012. doi:10.1523/JNEUROSCI.0669-12.2012.

Rainer G, Asaad WF, Miller EK. Selective representation of relevant information by neurons in the primate prefrontal cortex. *Nature* 393: 577–579, 1998. doi:10.1038/31235.

Roper SD. Taste buds as peripheral chemosensory processors. *Semin Cell Dev Biol* 24: 71–79, 2013. doi:10.1016/j.semcdb.2012.12.002.

Rosen AM, Roussin AT, Di Lorenzo PM. Water as an independent taste modality. *Front Neurosci* 4: 175, 2010. doi:10.3389/fnins.2010.00175.

Rosen AM, Victor JD, Di Lorenzo PM. Temporal coding of taste in the parabrachial nucleus of the pons of the rat. *J Neurophysiol* 105: 1889–1896, 2011. doi:10.1152/jn.00836.2010.

Roussin AT, D'Agostino AE, Fooden AM, Victor JD, Di Lorenzo PM. Taste coding in the nucleus of the solitary tract of the awake, freely licking rat. *J Neurosci* 32: 10494–10506, 2012. doi:10.1523/JNEUROSCI.1856-12.2012.

Sadacca BF, Rothwax JT, Katz DB. Sodium concentration coding gives way to evaluative coding in cortex and amygdala. *J Neurosci* 32: 9999–10011, 2012. doi:10.1523/JNEUROSCI.6059-11.2012.

Saddoris MP, Holland PC, Gallagher M. Associatively learned representations of taste outcomes activate taste-encoding neural ensembles in gustatory cortex. *J Neurosci* 29: 15386–15396, 2009. doi:10.1523/JNEUROSCI.3233-09.2009.

Samuelsen CL, Gardner MPH, Fontanini A. Effects of cue-triggered expectation on cortical processing of taste. *Neuron* 74: 410–422, 2012. doi:10.1016/j.neuron.2012.02.031.

Schroeder CE, Wilson DA, Radman T, Scharfman H, Lakatos P. Dynamics of active sensing and perceptual selection. *Curr Opin Neurobiol* 20: 172–176, 2010. doi:10.1016/j.conb.2010.02.010.

Shusterman R, Smear MC, Koulakov AA, Rinberg D. Precise olfactory responses tile the sniff cycle. *Nat Neurosci* 14: 1039–1044, 2011. doi:10.1038/nn.2877.

Simon SA, de Araujo IE, Gutierrez R, Nicolelis MA. The neural mechanisms of gustation: a distributed processing code. *Nat Rev Neurosci* 7: 890–901, 2006. doi:10.1038/nrn2006.

Smith DV, Travers JB. A metric for the breadth of tuning of gustatory neurons. *Chem Senses* 4: 215–229, 1979. doi:10.1093/chemse/4.3.215.

Spector AC, Klumpp PA, Kaplan JM. Analytical issues in the evaluation of food deprivation and sucrose concentration effects on the microstructure of licking behavior in the rat. *Behav Neurosci* 112: 678–694, 1998. doi:10.1037/0735-7044.112.3.678.

Spector AC, Travers SP. The representation of taste quality in the mammalian nervous system. *Behav Cogn Neurosci Rev* 4: 143–191, 2005. doi:10.1177/1534582305280031.

Stapleton JR, Lavine ML, Nicolelis MA, Simon SA. Ensembles of gustatory cortical neurons anticipate and discriminate between tastants in a single lick. *Front Neurosci* 1: 161–174, 2007. doi:10.3389/neuro.01.1.1.012.2007.

Stapleton JR, Lavine ML, Wolpert RL, Nicolelis MA, Simon SA. Rapid taste responses in the gustatory cortex during licking. *J Neurosci* 26: 4126–4138, 2006. doi:10.1523/JNEUROSCI.0092-06.2006.

Travers JB, Dinardo LA, Karimnamazi H. Motor and premotor mechanisms of licking. *Neurosci Biobehav Rev* 21: 631–647, 1997. doi:10.1016/S0149-7634(96)00045-0.

Verhagen JV, Giza BK, Scott TR. Responses to taste stimulation in the ventroposteromedial nucleus of the thalamus in rats. *J Neurophysiol* 89: 265–275, 2003. doi:10.1152/jn.00870.2001.

Vincis R, Chen K, Czarnecki L, Chen J, Fontanini A. Dynamic representation of taste-related decisions in the gustatory insular cortex of mice (Preprint). *bioRxiv* 878553, 2019. doi:10.1101/2019.12.16.878553

Vincis R, Fontanini A. A gustocentric perspective to understanding primary sensory cortices. *Curr Opin Neurobiol* 40: 118–124, 2016a. doi:10.1016/j.conb.2016.06.008.

Vincis R, Fontanini A. Associative learning changes cross-modal representations in the gustatory cortex. *eLife* 5: e16420, 2016b. doi:10.7554/eLife.16420.

Wachowiak M. All in a sniff: olfaction as a model for active sensing. *Neuron* 71: 962–973, 2011. doi:10.1016/j.neuron.2011.08.030.

Wang L, Gillis-Smith S, Peng Y, Zhang J, Chen X, Salzman CD, Ryba NJ, Zuker CS. The coding of valence and identity in the mammalian taste system. *Nature* 558: 127–131, 2018. doi:10.1038/s41586-018-0165-4.

Weiss MS, Victor JD, Di Lorenzo PM. Taste coding in the parabrachial nucleus of the pons in awake, freely licking rats and comparison with the nucleus of the solitary tract. *J Neurophysiol* 111: 1655–1670, 2014. doi:10.1152/jn.00643.2013.

Wilson DM, Lemon CH. Modulation of central gustatory coding by temperature. *J Neurophysiol* 110: 1117–1129, 2013. doi:10.1152/jn.00974.2012.

Yoshida T, Katz DB. Control of prestimulus activity related to improved sensory coding within a discrimination task. *J Neurosci* 31: 4101–4112, 2011. doi:10.1523/JNEUROSCI.4380-10.2011.

Zocchi D, Wennemuth G, Oka Y. The cellular mechanism for water detection in the mammalian taste system. *Nat Neurosci* 20: 927–933, 2017. doi:10.1038/nn.4575.